Engineered temperature compensation in a synthetic genetic clock

Faiza Hussain[a], Chinmaya Gupta[b], Andrew J. Hirning[a], William Ott[b], Kathleen S. Matthews[a,c], Krešimir Josić[b,d], and Matthew R. Bennett[a,c,1]

[a]Department of Biochemistry and Cell Biology, Rice University, Houston, TX 77005; [b]Department of Mathematics, University of Houston, Houston, TX 77204; [c]Institute of Biosciences and Bioengineering, Rice University, Houston, TX 77005; and [d]Department of Biology & Biochemistry, University of Houston, Houston, TX 77204

Edited by Joseph S. Takahashi, Howard Hughes Medical Institute, University of Texas Southwestern Medical Center, Dallas, TX, and approved December 13, 2013 (received for review September 6, 2013)

Synthetic biology promises to revolutionize biotechnology by providing the means to reengineer and reprogram cellular regulatory mechanisms. However, synthetic gene circuits are often unreliable, as changes to environmental conditions can fundamentally alter a circuit's behavior. One way to improve robustness is to use intrinsic properties of transcription factors within the circuit to buffer against intra- and extracellular variability. Here, we describe the design and construction of a synthetic gene oscillator in *Escherichia coli* that maintains a constant period over a range of temperatures. We started with a previously described synthetic dual-feedback oscillator with a temperature-dependent period. Computational modeling predicted and subsequent experiments confirmed that a single amino acid mutation to the core transcriptional repressor of the circuit results in temperature compensation. Specifically, we used a temperature-sensitive lactose repressor mutant that loses the ability to repress its target promoter at high temperatures. In the oscillator, this thermoinduction of the repressor leads to an increase in period at high temperatures that compensates for the decrease in period due to Arrhenius scaling of the reaction rates. The result is a transcriptional oscillator with a nearly constant period of 48 min for temperatures ranging from 30 °C to 41 °C. In contrast, in the absence of the mutation the period of the oscillator drops from 60 to 30 min over the same temperature range. This work demonstrates that synthetic gene circuits can be engineered to be robust to extracellular conditions through protein-level modifications.

LacI | circadian oscillator | microfluidics | cellular dynamics | delay

One major goal of synthetic biology is the creation of gene circuits that generate dynamic and programmable phenotypes within cells (1). Synthetic biologists have constructed a wide variety of synthetic gene circuits, including switches (2–4), logic gates (5–8), oscillators (9–11), and light-sensitive networks (12). Often, these circuits are built from genetic parts that regulate protein production, either at the transcriptional or translational level (13, 14). These engineered systems have revealed much about how a circuit's topology impacts its behavior (15). However, the creation of circuits that are robust to variations in environmental conditions remains a major challenge (16–18).

Temperature is one important environmental factor known to significantly alter gene circuit behavior (19). Biochemical reaction rates approximately double with every 10 °C increase in temperature (20), resulting in faster dynamical processes within the cell. Previous work has shown that the period of a synthetic dual-feedback oscillator in *Escherichia coli* is sensitive to temperature changes (19). As expected, the period of the oscillator roughly halves with a 10 °C increase in temperature. In contrast, naturally occurring circadian oscillators are robust to thermal variations and maintain a 24-h period over a range of physiologically relevant temperatures (21–25).

In circadian oscillators, the mechanisms underlying temperature compensation, i.e., the ability to maintain a constant period over a range of temperatures, are still unknown. However, several hypotheses have emerged based on theoretical and experimental evidence (26, 27). Hastings and Sweeney presented the simplest theoretical model for temperature compensation wherein opposing biochemical reactions form a feedback loop that maintains the pace of the clock (24). This model has been used to explain the *Arabidopsis thaliana* clock-associated feedback loops (23). In bacteria, a recent theoretical model indicates that the inherent properties of multisubstrate enzyme kinetics can lead to temperature compensation (28). Others have computationally evolved theoretical models to better understand the phenomenon (29).

Instead of trying to determine how native circadian oscillators compensate for temperature, in this study we forward-engineered thermal robustness into an existing synthetic gene oscillator (19). We used a synthetic circuit with a coupled positive and negative feedback topology that has been shown to oscillate in both bacteria and mammalian cells (11, 19), and is more tunable than other oscillator designs (30). Additionally, dual-feedback oscillators have previously been used to mimic other naturally occurring oscillatory phenomena such as environmental entrainment (31, 32) and intercellular synchronization of oscillations (33).

The dual-feedback oscillator used in this study is comprised of genes encoding the activator AraC, the repressor LacI, and a GFP reporter, as shown in Fig. 1*A*. All three genes are transcriptionally regulated by the $P_{lac/ara}$ hybrid promoter, which is repressed by LacI in the absence of isopropyl β-D-1-thiogalactopyranoside

Significance

Synthetic gene circuits are often fragile, as perturbations to cellular conditions frequently alter their behavior. This lack of robustness limits the utility of engineered gene circuits and hinders advances in synthetic biology. Here, we demonstrate that environmental sensitivity can be reduced by simultaneously engineering circuits at the protein and network levels. Specifically, we designed and constructed a synthetic genetic clock that exhibits temperature compensation—the clock's period does not depend on temperature. This feature is nontrivial since biochemical reactions speed up with increasing temperature. To accomplish this goal, we engineered thermal-inducibility into the clock's regulatory structure. Computational modeling predicted and experiments confirmed that this thermal-inducibility results in a clock with a stable period across a large range of temperatures.

Author contributions: F.H., K.S.M., K.J., and M.R.B. designed research; F.H., C.G., A.J.H., and W.O. performed research; F.H., C.G., W.O., and M.R.B. analyzed data; A.J.H. contributed new reagents/analytic tools; and F.H., C.G., A.J.H., K.J., and M.R.B. wrote the paper.

This article is a PNAS Direct Submission.

[1]To whom correspondence should be addressed. E-mail: matthew.bennett@rice.edu.

This article contains supporting information online at www.pnas.org/lookup/suppl/doi:10.1073/pnas.1316298111/-/DCSupplemental.

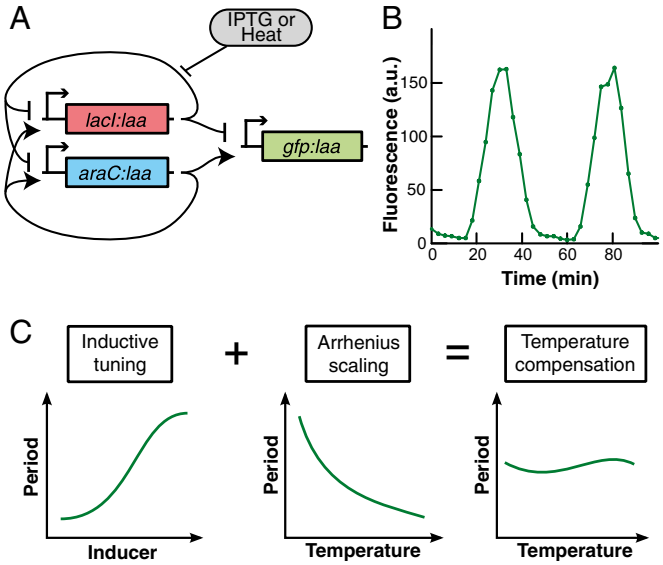

Fig. 1. A path to temperature compensation in the synthetic dual-feedback oscillator. (*A*) Circuit topology of the oscillator. The transcription factors AraC and LacI provide positive and negative feedback, respectively, and circuit dynamics are measured by GFP. All three genes have an ssrA tag to increase degradation rates. (*B*) GFP fluorescence of the circuit as a function of time in an individual cell. (*C*) Temperature compensation should be possible through a combination of inductive tuning (which increases the period) and Arrhenius scaling (which decreases the period).

(IPTG) and activated by AraC in the presence of arabinose (34). Each gene is also fused to a C-terminal *ssrA* degradation tag, consisting of the amino acids AANDENYALAA, which target proteins to the ClpXP protease degradation pathway in *E. coli*. The circuit generates sustained oscillations of a GFP reporter (19), as shown in Fig. 1*B*.

It is important to note that the period of the LacI–AraC dual-feedback oscillator is tunable through the titration of either arabinose or IPTG, the ligands of AraC and LacI, respectively. Stricker et al. found that concentrations of IPTG or arabinose that led to increased induction of the target promoter lead to an increase in the period of the oscillator (19). In other words, higher induction levels lead to longer periods. However, altering the ambient temperature from 25 °C to 37 °C resulted in a decrease in period length that was explained by the Arrhenius scaling of the reaction rates (19).

Given the opposing effects of induction (period increase) and temperature (period decrease) on period length, we hypothesized that temperature-dependent induction of a LacI-regulated promoter could stabilize oscillator period (Fig. 1*C*). Specifically, if LacI loses its ability to repress at high temperatures instead of high IPTG concentrations, then an increase in period due to thermal induction will counteract the decrease in period due to Arrhenius scaling of the reaction rates.

Here we show that thermal sensitivity of the repressor leads to temperature compensation in the dual-feedback oscillator. We first examined a temperature-sensitive mutant of LacI to show that heat can induce downstream transcription. Next, we used computational modeling to examine how the temperature-sensitive LacI mutant will alter the behavior of the dual-feedback oscillator and lead to temperature compensation. Finally, we placed the mutant into the oscillator and used time-lapse fluorescence microscopy to examine the dynamics of the mutant oscillator at the single-cell level and at various temperatures. As predicted, the dual-feedback oscillator maintains a nearly constant period over a wide range of physiologically relevant temperatures when it contains a temperature-sensitive repressor.

Results

Temperature-Dependent Induction of LacI. LacI has long been studied as a paradigm for transcriptional regulation of genes and much is known about its structure (35). In numerous studies, the gratuitous inducer, IPTG, which cannot be metabolized by *E. coli* has been used in place of the natural inducer, allolactose. However, several temperature-sensitive (ts) variants of LacI that are induced by heat rather than chemicals have been discovered.

We first examined the in vivo behavior of a temperature-sensitive variant of LacI that is induced by heat rather than IPTG. This variant (tsLacI) contains a glycine-to-serine mutation at position 187 and fully represses transcriptional activity at 30 °C, but undergoes full induction at 42 °C, even in the absence of chemical inducers (36). Based on crystal structures, position 187 is situated in a domain crossover in close proximity to the IPTG-binding pocket, and substitution at this position possibly introduces greater flexibility with an increase in temperature. Flexibility in this region has been shown to play a vital role in the allosteric response elicited as structural transition in the protein upon inducer binding (37). Thus, we created a LacI-inducible expression system to validate the thermal inducibility of tsLacI and compare its repressional activity to wild-type LacI (wtLacI) as a function of temperature. We cloned the *lacI* genes (wt or ts) into the pZSlacI plasmid under the constitutive *I* promoter. The reporter gene, *gfp*, was cloned into the pGFPkan plasmid under the transcriptional control of the P_{LlacO1} promoter (34) (Fig. 2 *A* and *B*). The plasmids were cotransformed into the Δ*araC*Δ*lacI* *E. coli* strain, JS006 (19).

We next examined the inducibility of genes regulated by wtLacI by growing cells cotransformed with pZSlacI and pGFPkan at 37 °C in the presence of increasing concentrations of IPTG. As expected, IPTG induces transcription of genes regulated by wtLacI, evident

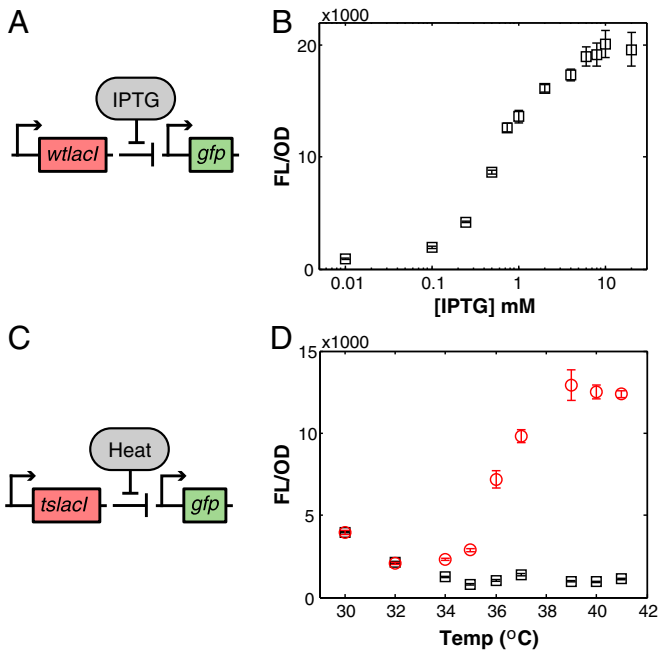

Fig. 2. Comparison of chemical and thermal induction of LacI systems. (*A*) Circuit diagram of an IPTG-inducible LacI system. (*B*) Relative fluorescence as a function of IPTG concentration for the wild-type system. (*C*) Circuit diagram of a heat-inducible LacI system. (*D*) Relative GFP fluorescence as a function of temperature for both the temperature sensitive (red circles) and the wild-type systems (black squares). Error bars represent SD.

here by an increase in GFP fluorescence (Fig. 2*B*). In contrast, genes regulated by tsLacI are induced by elevated temperature (Fig. 2*D*). This temperature sensitivity is absent in wtLacI as it fully represses transcription of *gfp* in the range of temperatures we tested (Fig. 2*D*).

Computational Modeling. To explore temperature compensation in the oscillator, we extended a previously reported computational model (38) to predict how temperature affects the period of an oscillator containing a temperature-sensitive *lacI* mutant. This computational model includes scaling of each reaction rate according to the Arrhenius Law. To model the effect of replacing wtLacI with a temperature-sensitive variant, we varied the repressor's affinity to operator so that it depends on temperature instead of IPTG concentration. Specifically, we modeled the dynamics of LacI and AraC with the delay differential equations **[1]** and **[2]**.

$$A(T)\cdot\frac{\mathrm{d}r}{\mathrm{d}t}=\frac{\alpha_r\left(f^{-1}+\frac{a(t-A(t)\cdot\tau_r)}{C_a}\right)}{\left(1+\frac{a(t-A(t)\cdot\tau_r)}{C_a}\right)\left(1+\frac{r(t-A(t)\cdot\tau_r)}{C_r(T)}\right)^N}-\beta r(t)-\frac{\gamma_r r(t)}{R_0+r(t)+a(t)} \quad [1]$$

$$A(T)\cdot\frac{\mathrm{d}a}{\mathrm{d}t}=\frac{\alpha_a\left(f^{-1}+\frac{a(t-A(t)\cdot\tau_a)}{C_a}\right)}{\left(1+\frac{a(t-A(t)\cdot\tau_a)}{C_a}\right)\left(1+\frac{r(t-A(t)\cdot\tau_a)}{C_r(T)}\right)^N}-\beta a(t)-\frac{\gamma_a a(t)}{R_0+r(t)+a(t)}, \quad [2]$$

In our model, $r(t)$ and $a(t)$ are the concentrations at time t of LacI and AraC, respectively; τ_r and τ_a are the transcriptional delay times of the LacI and AraC, respectively; α_r and α_a are the maximal transcription rates of LacI and AraC, respectively; f is a unitless measure of the strength of the positive feedback loop; C_a is the concentration of AraC needed to provide half-maximal induction; $C_r(T)$ is the temperature-dependent concentration of LacI needed for half-maximal repression; N is the Hill coefficient for LacI repression; β is the dilution-rate constant due to cellular growth and division; γ_r, γ_a, and R_0 are the Michaelis–Menten constants for the coupled enzymatic decay of LacI and AraC; $A(T)$ is the Arrhenius scaling term; T is the temperature; and the overdot represents differentiation with respect to time. The Arrhenius scaling term, $A(T)$ is given by

$$A(T)=\exp\left\{\theta\left[\frac{1}{T+273}-\frac{1}{T_{ref}+273}\right]\right\}, \quad [3]$$

where θ is the Arrhenius constant for the system and T_{ref} is the reference temperature. To model the temperature sensitivity of tsLacI, we defined $C_r(T)$ to be a Hill function of the form

$$C_r(T)=\left(C_{r,max}-C_{r,min}\right)\frac{\left(\frac{T}{T_0}\right)^b}{1+\left(\frac{T}{T_0}\right)^b}+C_{r,min}, \quad [4]$$

where $C_{r,min}$ and $C_{r,max}$ are minimum and maximum values of $C_r(T)$, respectively, T_0 is the temperature at which $C_r(T)$ is half-maximal, and b is a Hill coefficient. Note that the enzymatic decay of each protein depends on the concentration of both, because both AraC and LacI are targeted by the same protease (39). All parameter values are provided in the Table S1.

To approximate and fit the temperature dependence of tsLacI in the induction experiments we assumed that the relative induction level was given by the proportion

$$I(T)\propto\frac{1}{1+\left(\frac{[LacI]}{C_r(T)}\right)^N}, \quad [5]$$

where $I(T)$ is the induction level as a function of the temperature, T, and the steady-state level of LacI was chosen to be $[LacI]=300$ molecules/cell.

Fig. 3 shows results of the computational model using a set of parameters that provide good agreement with wild-type oscillator and a reasonable approximation of the thermal inducibility of the temperature-compensating oscillator. The model predicts that when tsLacI is used in place of wtLacI the period of the oscillator is far lass sensitive to the ambient temperature. Further computational modeling predicts that temperature compensation should exist for a wide range of parameters (*Supporting Information* and Fig. S1). This suggests that this mechanism of temperature compensation is quite robust.

Single-Cell Dynamics of the Oscillator at Various Temperatures. Given the observed IPTG and temperature dependence for wtLacI and tsLacI, we used microfluidics in conjunction with time-lapse fluorescence microscopy to examine the temporal changes in gene expression in the dual-feedback oscillator (40). The periodic induction of GFP synthesis allows monitoring the state of the oscillator circuit in individual cells. We transformed the oscillator plasmids containing either *wtlacI* or *tslacI* into *E. coli* JS006 cells and used individual colonies to inoculate fresh Luria Bertani (LB) media supplemented with antibiotics for overnight growth at 30 °C. The next day, the overnight cultures were used to inoculate fresh LB media supplemented with antibiotics and grown at the desired temperature without addition of chemical inducers. No lethality to the *E. coli* cells was observed for the ts variant as indicated by the overlap in growth curves of the oscillators containing either wt or ts *lacI* (Fig. S2). Doubling times of the cultures ranged from ∼36 min at 30 °C to 21 min at 41 °C for both versions of the oscillator. Cells were grown in an incubator/shaker until the optical density at 600 nm reached ∼0.15. They were then transferred to a microfluidic device with a trapping region that allows *E. coli* cells to grow in a monolayer, as shown in Fig. 4*A*.

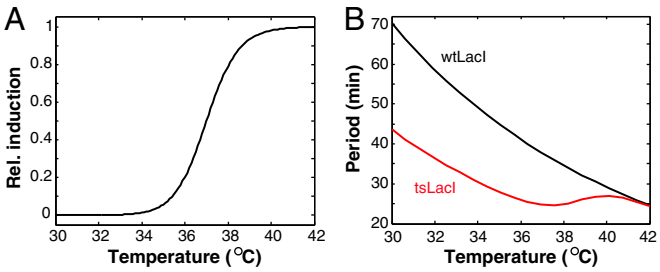

Fig. 3. Prediction of a computational model of the dual-feedback oscillator containing a temperature sensitive LacI mutant. (*A*) The Hill function of a tsLacI-regulated promoter. Shown is the relative induction level as a function of temperature. (*B*) The period of the dual-feedback oscillator as a function of temperature for circuits containing either wild-type (black curve) or temperature sensitive lacI (red curve).

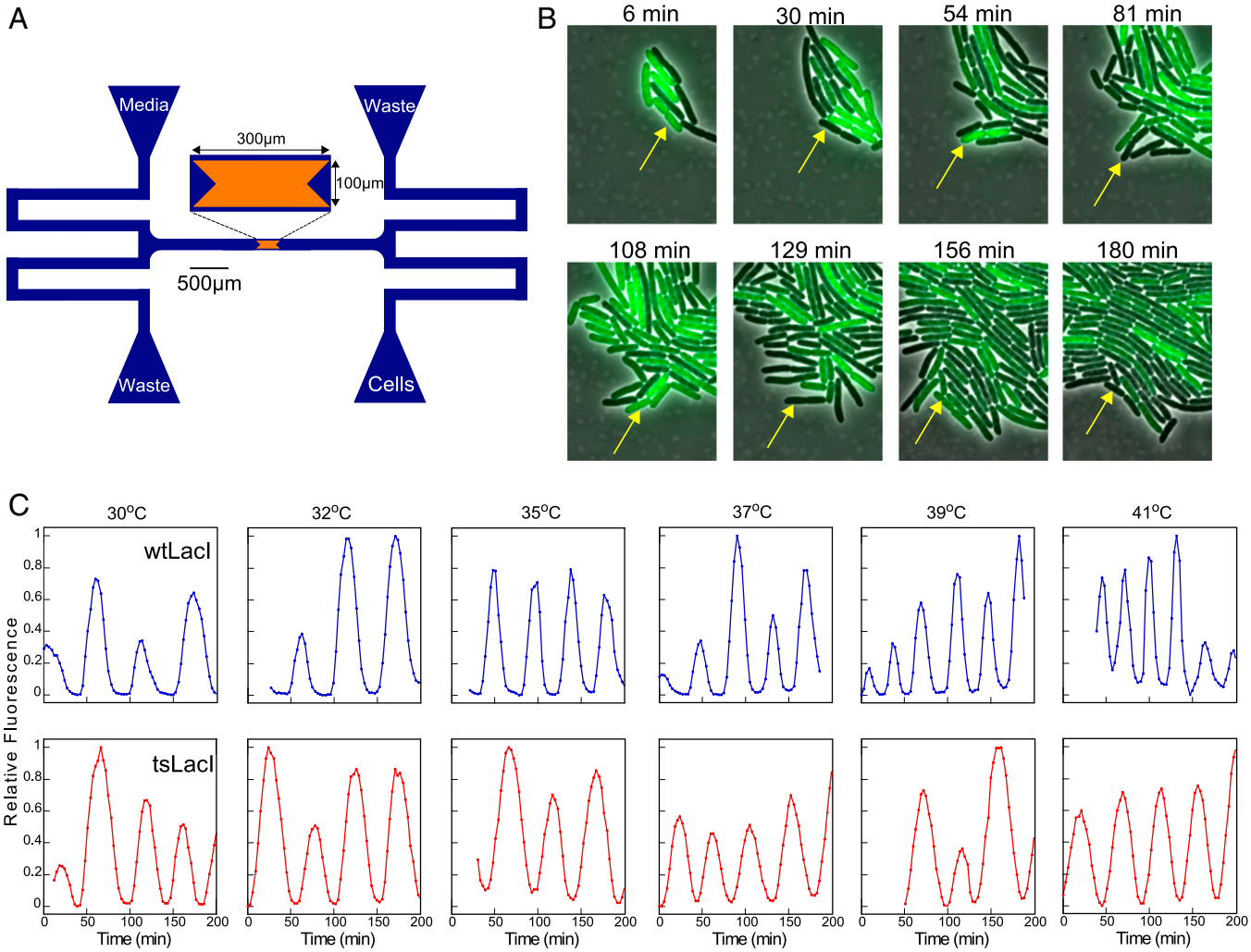

Fig. 4. Tracking the oscillator at the single-cell level. (*A*) Schematic of the microfluidic device used for time-lapse fluorescence microscopy in this study. Triangular regions are fluid line ports for cells, media, and waste. An enlargement of the cell trapping region is shown. The blue area has a 5-μm channel height, and the yellow area has a 0.95-μm channel height. The trap is 300 μm long and 100 μm wide. (*B*) Images of *E. coli* cells in the microfluidic device at different time points. The yellow arrows point to the same cell in each image. Each image is a combination of the phase contrast and green fluorescence channels. (*C*) Representative GFP trajectories of individual cells at varying temperatures for the dual feedback oscillator containing wtLacI (blue, *Upper*) or tsLacI (red, *Lower*).

We cultivated the dual-feedback oscillator with the wtlacI gene at various temperatures in a microfluidic device with a constant fresh LB media source supplemented with 0.7% arabinose and 2 mM IPTG. The aforementioned inducer concentrations have previously been shown to optimally induce *gfp* expression in almost all observed cells (19). The tsLacI oscillator was cultivated at several temperatures but only in the presence of 0.7% arabinose. Cells with each type of LacI variant were grown for several hours in the microfluidic device with controlled ambient temperature. Next, we measured the time-dependent fluorescence of individual cells of both variants over several generations at each cultivation temperature (Fig. 4*B*). For each scope run at the desired temperature, we tracked 8–10 cells over multiple generations (at least 7). The raw data for representative runs for wtLacI and tsLacI ranging from 30 °C to 41 °C shows persistent periodic oscillations for both variants (Fig. 4*C*).

Fig. 5 summarizes the results. The temperature-dependent induction of the ts mutant is shown in Fig. 5*A*. In Fig. 5 *B* and *C*, the average period of the oscillator with wtLacI and tsLacI, respectively, is plotted as a function of temperature. In each of these, we also show results of our mathematical model after fitting the parameters to the data. As predicted by the computational model, the period of the wild-type oscillator is halved as the temperature is increased by 10 °C; whereas, the period of the tsLacI oscillator remains nearly unchanged even at high temperatures. Thus, thermal induction of the repressor buffered the effects of temperature variability in the dual-feedback oscillator.

Discussion

As with all engineered devices, synthetic gene circuits must be robust to provide practical benefits. Synthetic biologists are now facing robustness problems similar to those faced by mechanical engineers and control theorists. In fact, temperature compensation has a long history in the engineering of devices for accurate timekeeping. For instance, changes in temperature alter the length of the pendulum rod of pendulum clocks, changing the period of a swing (41). Similarly, a working solution to the longitude problem required robust temperature compensation. John Harrison, the inventor of the marine chronometer, was famously able to compensate for thermal expansion of a clock's components by using a bimetallic rod (42).

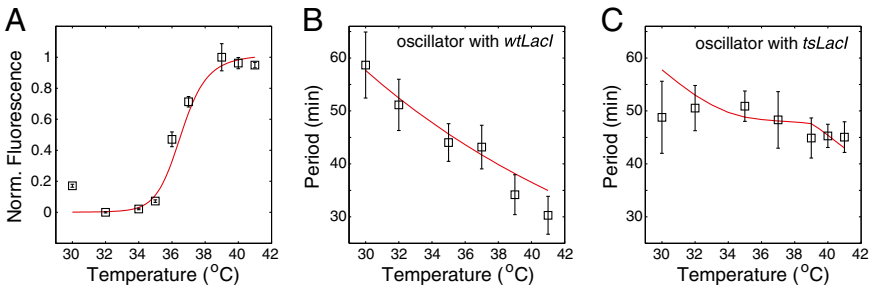

Fig. 5. Comparison of experimental and computational results for the temperature-compensating oscillator. (*A*) Relative fluorescence as a function of temperature for the tsLacI-induction experiments (black squares) and the model fit (red curve). The experimental data here are the same as shown in Fig. 2*D*. Note that the model predicts that no induction occurs at any temperature if wtLacI is used instead of tsLacI, and hence is not shown here. (*B* and *C*) Experimentally measured period (black squares) and model fit (red curve) of the wild-type and temperature-compensating oscillator as a function of temperature, respectively. Error bars represent SD.

Although rational design will provide solutions to the robustness problem in synthetic biology, evolution has already solved many of the same problems in living organisms. Such solutions could be emulated to create synthetic gene circuits that are robust to a wide range of environmental perturbations. For instance, new insights into temperature compensation might be gained from circadian oscillators themselves (27, 43–47).

Although we have successfully forward-engineered temperature compensation into a synthetic oscillator, we do not claim to have elucidated the mechanisms of temperature compensation in naturally occurring circadian oscillators. However, some evidence suggests that the mechanism that imparts robustness to our synthetic oscillator (i.e., thermoinduction of the core repressor) is similar to mechanisms seen in circadian oscillators. For instance, in *Neurospora crassa*, the FRQ protein forms the core of the circadian clock's negative feedback loop (similar to LacI in our oscillator). Experimental evidence suggests that the thermal stability of the protein and the temperature dependent splicing of its mRNA play an important role in temperature compensation (45, 46). Simple mathematical models based on Goodwin's oscillator (45, 48) have already shown that these mechanisms can impart temperature compensation. Similarly in mammalian circadian clocks, the *Per1* gene provides negative feedback and has been implicated in temperature compensation (49). Computational studies have also shown that the degradation rate of *Per* mRNA affects the period of the clock (50). It would therefore be interesting to see if thermoinduction could also impart temperature compensation in models of circadian oscillators.

Finally, the temperature compensation exhibited by this oscillator is the result of counteracting effects of inductive tuning and Arrhenius scaling. These two phenomena passively combine to create an oscillator that has a constant period over a wide range of physiologically relevant temperatures. It is important to note that this robustness is a consequence of a single amino acid change to a constituent regulatory protein and not to the overall topology of the circuit. Therefore, our study sets the stage for further investigations into the multiscale relationship between protein structure/function and the dynamics of synthetic gene circuits.

Materials and Methods

LacI-Inducible Expression System. The pZSlacI plasmid was created by modifying the pzs4intLacITetR plasmid purchased from Expressys. The P_{N25} promoter, *tetR* gene, and *attP* site were deleted from the plasmid using site-directed mutagenesis; spectinomycin resistance gene was swapped out with the beta-lactamase gene for ampicillin resistance. The constitutive Iq promoter driving expression of the lacI repressor was changed to the *I* promoter using site-directed mutagenesis (*Supporting Information*). The *wtlacI* gene was used as the parental template to generate the G187S *lacI* variant (*tslacI*). The reporter gene, *gfp*, was cloned downstream of the PLlac01 promoter in the reporter plasmid. The *ssrA* degradation tag was inserted at the C terminus of the *gfp* gene. The reporter module, pGFPKan, contains a kanamycin-resistance marker.

Induction Curves. The repressor plasmid, pZSlacI, and reporter plasmid, pGFPKan, were cotransformed into the JS006 Δ*ara*Δ*lacI E. coli* strain. Single colonies were used to inoculate 5 mL LB media supplemented with 100 μg/mL ampicillin and 50 μg/mL kanamycin and grown overnight at 30 °C. The next morning, fresh 5 mL LB cultures supplemented with antibiotics were inoculated with overnight cultures at 1:100 dilution. Cultures were grown at the desired temperature in an incubator/shaker and harvested following 3 h of growth. Cells were plated in triplicate in a 96-well BD-Falcon plate. The optical density at 600 nm and fluorescence (λ excitation = 490 nm and λ emission = 510 nm) were measured using a Perkin–Elmer plate reader. As positive control of the LacI-inducible expression system, cells with the wild-type repressor were grown at 37 °C in presence of different concentrations of IPTG.

Dual-Feedback Oscillator Plasmids. The plasmids pJS167NheI and pZA14LacI for the wild-type dual-feedback oscillators were obtained from the Hasty laboratory (19). Both the activator, *araC*, and reporter, *gfp*, genes were cloned in the pJS167NheI plasmid under the control of the $P_{lac/ara}$ hybrid promoter with a selectable marker for kanamycin. The repressor gene, *lacI*, was also placed under the control of the $P_{lac/ara}$ hybrid promoter in the ampicillin-resistant pZA14LacI plasmid. The plasmids were cotransformed in JS006. Plasmid maps and detailed descriptions of each plasmid used in this study are provided in Fig. S3 and Table S2.

Microscopy. The activator (pJS167NheI) and repressor (pZA14LacI) plasmids were cotransformed into the Δ *araC*Δ*lacI* double knockout *E. coli* strain, JS006, and plated on agar plates supplemented with 100 μg/mL amp and 50 μg/mL kan. Plates were incubated at 37 °C overnight and placed at 4 °C until inoculation of liquid cultures. Single colonies were picked for inoculation of 5 mL LB supplemented with 100 μg/mL ampicillin and 50 μg/mL kanamycin and grown overnight at 30 °C in an incubator/shaker. The next morning, fresh 25 mL LB with amp/kan was inoculated with 25 μL of the overnight culture and grown in the incubator/shaker preset to the desired temperature. Optical density of the cultures was monitored periodically by removing a 500 μL aliquot of the culture and measuring absorbance at 600 nm. Cells were harvested at an absorbance of ~0.15 by removing 10 mL of the culture and centrifuging at 3,500 rpm for 5 min. The medium was discarded, and fresh 10 mL LB media with antibiotics was used to resuspend the cells before loading on a microfluidic device.

The fluorescence microscope (Nikon, Inc.) was encased in a Plexiglas assembly connected to a heating element with variable temperature settings to ensure cells grow at a stable temperature. An hour before loading cells on the microfluidic device, the device was flushed with 0.1% Tween 20 (Sigma-Aldrich) to remove residual polydimethylsiloxane (PDMS) debris. Postflushing, a media syringe containing 10 mL LB, antibiotics, and 0.7% arabinose (plus 2 mM IPTG for wtLacI) was connected to the media port in the device with Tygon plastic flexible tubing (Norton Performance Plastics) and a 23-gauge Luer stub adapter. Two additional syringes containing sterilized water were connected to the waste ports in the device; the waste ports allow for removal of untrapped cells during loading as well as removal of surplus media to prohibit contamination. The cell culture was loaded in a syringe

and connected to the cell port on the microfluidic device. Cells were trapped into the 1-μm trapping region by "flicking" the plastic tubing until one or two cells were trapped in the trapping region. The flow of the syringes was then reversed, with the media syringe situated at a greater height than the cell syringe to ensure constant media flow to the device. Cells in the trapping region were grown for at least 7 h and imaged every 3 min with the 100× phase contrast (600-ms exposure time) and GFP fluorescent channels (300-ms exposure time) using a Nikon camera installed in the microscope. The focus was maintained by an automated contrast-based autofocus function.

Image Analysis. The microscope runs were analyzed with the Wright Cell Imaging Facility ImageJ cell analysis software package (Wayne Rasband, Research Services Branch, National Institute of Mental Health with plug-in collation and organization by the Wright Cell Imaging Facility). Images from the phase-contrast channel were used to outline individual *E. coli* cells as ellipses for tracking over several generations. The phase-contrast images were overlaid on the fluorescence channel images to measure the mean fluorescence of the outlined individual cell. The mean fluorescence (averaged over pixels) of each single cell was measured for 7–12 generations and plotted as a function of time; the distance from one peak to the next was measured and reported as period duration. Successive periods were measured and averaged for each individual cell tracked and plotted as a function of temperature.

Methods and supporting data, including representative movies of the oscillators, are provided in the *Supporting Information*.

ACKNOWLEDGMENTS. We thank Jeff Hasty for providing us with the original oscillator plasmids. This work was funded by the National Institutes of Health, through the joint National Science Foundation/National Institute of General Medical Sciences Mathematical Biology Program Grant R01GM104974 (to M.R.B., K.J., and W.O.), the Robert A. Welch Foundation Grants C-1729 (to M.R.B.) and C-576 (to K.S.M.), and the John S. Dunn Foundation Collaborative Research Award Program administered by the Gulf Coast Consortia (M.R.B. and K.J.).

1. Khalil AS, Collins JJ (2010) Synthetic biology: Applications come of age. *Nat Rev Genet* 11(5):367–379.
2. Gardner TS, Cantor CR, Collins JJ (2000) Construction of a genetic toggle switch in Escherichia coli. *Nature* 403(6767):339–342.
3. Kim J, White KS, Winfree E (2006) Construction of an in vitro bistable circuit from synthetic transcriptional switches. *Mol Syst Biol* 2:68.
4. Wu M, et al. (2013) Engineering of regulated stochastic cell fate determination. *Proc Natl Acad Sci USA* 110(26):10610–10615.
5. Ausländer S, Ausländer D, Müller M, Wieland M, Fussenegger M (2012) Programmable single-cell mammalian biocomputers. *Nature* 487(7405):123–127.
6. Regot S, et al. (2011) Distributed biological computation with multicellular engineered networks. *Nature* 469(7329):207–211.
7. Tamsir A, Tabor JJ, Voigt CA (2011) Robust multicellular computing using genetically encoded NOR gates and chemical 'wires' *Nature* 469(7329):212–215.
8. Shis DL, Bennett MR (2013) Library of synthetic transcriptional AND gates built with split T7 RNA polymerase mutants. *Proc Natl Acad Sci USA* 110(13):5028–5033.
9. Elowitz MB, Leibler S (2000) A synthetic oscillatory network of transcriptional regulators. *Nature* 403(6767):335–338.
10. Fung E, et al. (2005) A synthetic gene-metabolic oscillator. *Nature* 435(7038):118–122.
11. Tigges M, Marquez-Lago TT, Stelling J, Fussenegger M (2009) A tunable synthetic mammalian oscillator. *Nature* 457(7227):309–312.
12. Levskaya A, Weiner OD, Lim WA, Voigt CA (2009) Spatiotemporal control of cell signalling using a light-switchable protein interaction. *Nature* 461(7266):997–1001.
13. Callura JM, Cantor CR, Collins JJ (2012) Genetic switchboard for synthetic biology applications. *Proc Natl Acad Sci USA* 109(15):5850–5855.
14. Mutalik VK, et al. (2013) Precise and reliable gene expression via standard transcription and translation initiation elements. *Nat Methods* 10(4):354–360.
15. Purcell O, Savery NJ, Grierson CS, di Bernardo M (2010) A comparative analysis of synthetic genetic oscillators. *J R Soc Interface* 7(52):1503–1524.
16. Hasty J, McMillen D, Collins JJ (2002) Engineered gene circuits. *Nature* 420(6912): 224–230.
17. Kaznessis YN (2007) Models for synthetic biology. *BMC Syst Biol* 1:47.
18. Randall A, Guye P, Gupta S, Duportet X, Weiss R (2011) Design and connection of robust genetic circuits. *Methods Enzymol* 497:159–186.
19. Stricker J, Cookson S, Bennett MR, Mather WH, Tsimring LS, Hasty J (2008) A fast, robust and tunable synthetic gene oscillator. *Nature* 456:516–519.
20. Segel IH (1975) *Enzyme kinetics: Behavior and analysis of rapid equilibrium and steady state enzyme systems* (Wiley, New York).
21. Baker CL, Loros JJ, Dunlap JC (2012) The circadian clock of Neurospora crassa. *FEMS Microbiol Rev* 36(1):95–110.
22. Dunlap JC (1999) Molecular bases for circadian clocks. *Cell* 96(2):271–290.
23. Gould PD, et al. (2006) The molecular basis of temperature compensation in the Arabidopsis circadian clock. *Plant Cell* 18(5):1177–1187.
24. Hastings JW, Sweeney BM (1957) On the mechanism of temperature independence in a biological clock. *Proc Natl Acad Sci USA* 43(9):804–811.
25. Winfree AT (1991) Circadian rhythms. Resetting the human clock. *Nature* 350(6313):18.
26. Pavlidis T, Zimmerman WF, Osborn J (1968) A mathematical model for the temperature effects on circadian rhythms. *J Theor Biol* 18(2):210–221.
27. Hong CI, Conrad ED, Tyson JJ (2007) A proposal for robust temperature compensation of circadian rhythms. *Proc Natl Acad Sci USA* 104(4):1195–1200.
28. Hatakeyama TS, Kaneko K (2012) Generic temperature compensation of biological clocks by autonomous regulation of catalyst concentration. *Proc Natl Acad Sci USA* 109(21):8109–8114.
29. François P, Despierre N, Siggia ED (2012) Adaptive temperature compensation in circadian oscillations. *PLOS Comput Biol* 8(7):e1002585.
30. Tsai TY-C, et al. (2008) Robust, tunable biological oscillations from interlinked positive and negative feedback loops. *Science* 321(5885):126–129.
31. Mondragón-Palomino O, Danino T, Selimkhanov J, Tsimring L, Hasty J (2011) Entrainment of a population of synthetic genetic oscillators. *Science* 333(6047):1315–1319.
32. Rodrigo G, Kirov B, Shen S, Jaramillo A (2013) Theoretical and experimental analysis of the forced LacI-AraC oscillator with a minimal gene regulatory model. *Chaos* 23(2): 025109.
33. Danino T, Mondragón-Palomino O, Tsimring L, Hasty J (2010) A synchronized quorum of genetic clocks. *Nature* 463(7279):326–330.
34. Lutz R, Bujard H (1997) Independent and tight regulation of transcriptional units in Escherichia coli via the LacR/O, the TetR/O and AraC/I1-I2 regulatory elements. *Nucleic Acids Res* 25(6):1203–1210.
35. Lewis M, et al. (1996) Crystal structure of the lactose operon repressor and its complexes with DNA and inducer. *Science* 271(5253):1247–1254.
36. Hasan N, Szybalski W (1995) Construction of lacIts and lacI^{q}ts expression plasmids and evaluation of the thermosensitive lac repressor. *Gene* 163(1):35–40.
37. Xu J, Matthews KS (2009) Flexibility in the inducer binding region is crucial for allostery in the Escherichia coli lactose repressor. *Biochemistry* 48(22):4988–4998.
38. Mather W, Bennett MR, Hasty J, Tsimring LS (2009) Delay-induced degrade-and-fire oscillations in small genetic circuits. *Phys Rev Lett* 102(6):068105.
39. Cookson NA, et al. (2011) Queueing up for enzymatic processing: Correlated signaling through coupled degradation. *Mol Syst Biol* 7:561.
40. Bennett MR, Hasty J (2009) Microfluidic devices for measuring gene network dynamics in single cells. *Nat Rev Genet* 10(9):628–638.
41. Graham G (1726) A contrivance to avoid irregularities in a clock's motion occasion'd by the action of heat and cold upon the rod of the pendulum. *Philos Trans Royal Soc* 34:392.
42. Sobel D (1995) *Longitude* (Walker & Company, New York).
43. James AB, et al. (2012) Alternative splicing mediates responses of the Arabidopsis circadian clock to temperature changes. *Plant Cell* 24(3):961–981.
44. Tseng YY, Hunt SM, Heintzen C, Crosthwaite SK, Schwartz JM (2012) Comprehensive modelling of the Neurospora circadian clock and its temperature compensation. *PLOS Comput Biol* 8(3):e1002437.
45. Ruoff P, Loros JJ, Dunlap JC (2005) The relationship between FRQ-protein stability and temperature compensation in the Neurospora circadian clock. *Proc Natl Acad Sci USA* 102(49):17681–17686.
46. Diernfellner A, et al. (2007) Long and short isoforms of Neurospora clock protein FRQ support temperature-compensated circadian rhythms. *FEBS Lett* 581(30):5759–5764.
47. Aronson BD, Johnson KA, Loros JJ, Dunlap JC (1994) Negative feedback defining a circadian clock: Autoregulation of the clock gene frequency. *Science* 263(5153): 1578–1584.
48. Forger DB (2011) Signal processing in cellular clocks. *Proc Natl Acad Sci USA* 108(11): 4281–4285.
49. Dibner C, et al. (2009) Circadian gene expression is resilient to large fluctuations in overall transcription rates. *EMBO J* 28(2):123–134.
50. Relógio A, et al. (2011) Tuning the mammalian circadian clock: Robust synergy of two loops. *PLOS Comput Biol* 7(12):e1002309.